ELSEVIER

International Journal of Heat and Fluid Flow 19 (1998) 159–166

International Journal of HEAT AND FLUID FLOW

Intercellular mass transfer in wavy/turbulent Taylor vortex flow

Naoto Ohmura [a,*], Tsukasa Makino [b], Atsushi Motomura [a], Yuichiro Shibata [a], Kunio Kataoka [a]

[a] *Department of Chemical Science and Engineering, Kobe University, Rokkodai, Nada, Kobe 657-8501, Japan*
[b] *KANEKA Corporation, Takasago 676-8688, Japan*

Received 29 August 1997; accepted 25 October 1997

Abstract

Axial mass transfer or mixing through trains of cellular vortices has been observed in the range of time-dependent wavy vortex flow with the aid of visualization technique of wave motion, salt-tracer response technique, and spectral analysis of fluctuating velocity-gradients. There appear multiple stable flow states even at the same Reynolds number owing to the hysteresis of the flow system, depending upon the start-up operation. Intercellular mass transfer depends upon the axial wavelength and wave motion as well as the Reynolds number in the range of singly (SPWVF) and doubly periodic wavy vortex flow (DPWVF) whereas it is controlled mainly by turbulent motion in the range of weakly turbulent wavy vortex (WTWVF) and fully turbulent Taylor vortex flows (TTVF). Intracellular mixing increases monotonically with Reynolds number, regardless of the flow state.

Keywords: Taylor vortex flow; Bifurcation; Hysteresis; Multiplicity; Wavy vortex flow; Turbulent vortex flow; Mass transfer; Intercellular mixing; Intracellular mixing

Notation

C	tracer concentration
D_z	effective axial diffusion coefficient
d	annular gap width
E	back-mixing coefficient
f, f_1, f_r	frequency, first-fundamental frequency, rotation frequency of inner cylinder
H	height of annular space
Re	Reynolds number based on inner cylinder rotation
R_i	radius of inner cylinder
t	time
z	axial coordinate
Γ	aspect ratio of annular space
λ	axial wavelength (axial height of one vortex)
ν	kinematic viscosity of fluid
ω	angular velocity of inner cylinder

1. Introduction

This paper deals experimentally with mass transfer through the trains of cellular vortices (“Taylor vortices”) formed in an annular gap between two concentric circular cylinders with the inner one rotating. This flow system experiences the following bifurcation scenario (Kataoka, 1986) of dynamical transitions as the Reynolds number is raised, i.e. (1) laminar Couette flow (LCF), (2) laminar Taylor vortex flow (LTVF), (3) singly periodic wavy vortex flow (SPWVF), (4) doubly periodic wavy vortex flow (DPWVF), (5) weakly turbulent wavy vortex flow (WTWVF), and (6) turbulent Taylor vortex flow (TTVF). The inflow cell boundaries where the secondary streams are directed towards the inner cylinder wall present a barrier to intercellular mass transfer between vortex pairs as compared to the outflow ones.

Therefore a pair of vortices separated by the inflow cell boundaries can be assumed as a mixing unit. If a small rate of axial flow is added constantly, trains of vortices will march through in single file without breakdown. This suggests the possibility that the residence time distribution of fluid elements within each pair of vortices can be controlled sharply (Kataoka et al., 1975; Kataoka and Takigawa, 1981; Pudjiono et al., 1992). Owing to the hysteresis of this flow system, there appear different flow states even at the same Reynolds number, depending upon how the steady state is reached (Ohmura et al., 1995). In a previous work (Kataoka et al., 1993), intermixing across cell boundaries was observed in the form of a mass-transfer coefficient (Kataoka and Takigawa, 1981; Ohmura et al., 1997a) defined at the interface between neighboring vortex pairs. At that time, however, the question of having to take into account the effect of vortex size and wave motion on the intermixing did not arise. In the present work, a

* Corresponding author.

0142-727X/98/$19.00
PII: S0142-727X(97)10020-0

computer-aided acceleration for the start-up operation was employed to specify the route leading to the steady operation of the inner cylinder rotation. The main purpose has been to observe mass transfer over wavy or turbulent cell boundaries in relation to the hysteresis of the flow system and the bifurcation of dynamical transition.

2. Experimental apparatus

As shown in Fig. 1, the experimental equipment consists of a transparent outer cylinder of acrylic resin (ID = 124 mm) and an inner cylinder of SUS (OD = 87.2 mm, i.e. $R_i = 43.6$ mm), giving an annular gap width d of 18.4 mm and an effective height H of 990 mm. The annular space was divided into three sections by inserting two ring-shaped partition disks (2 mm thick). The lower two sections were spaced with approximately equal aspect ratios, so that both of them could attain the same flow state. The aspect ratios $\Gamma = H/d$ of the two test sections were fixed to be approximately 20.0. An aqueous solution of glycerin was used as the working fluid. Taking into account the hysteresis of this flow system, two ways of starting up were adopted to reach the steady state rotation of the inner cylinder; (1) an impulsive start from rest to the steady rotation and (2) a gradual acceleration from rest at a specified constant rate until the steady rotation was reached.

Observations were made at steady-state operation with no axial flow. The cross-section of vortices visualized with poster color was observed, applying a plane sheet of laser light into the test section I shown in Fig. 2, in order to examine not only the vortex structure but also the wave motion of cell boundaries. The sequential visual data taken by a CCD camera were image-processed to get a clear picture of the waving cell boundaries.

A salt-solution tracer technique was utilized to measure the axial mass transfer over an inflow cell boundary as well as the peripheral mass transfer within a pair of vortices. A tracer injector and two Ni-electrodes of a conductivity cell were installed in the test section II shown in Fig. 3. As shown in the same figure, an inflow cell boundary is adjusted to lie between the two Ni-electrodes. The same working fluid was used as a tracer solution by adding a small amount of NaOH. The effective axial diffusion coefficient D_z, defined with a one-dimensional diffusion model (Tam and Swinney, 1987), was determined by a parameter-fitting method applied to the experimental plots of $\ln |C(z_1,t)/C(z_2,t)|$ vs. $1/t$, where $C(z_1,t)$ and $C(z_2,t)$ are the tracer concentration signals obtained from the two Ni-electrodes. Therefore this method can determine the axial diffusion over one inflow cell boundary between the two Ni-electrodes. A one-dimensional back-mixing model was utilized to determine peripheral back-mixing coefficient E within a pair of vortices. The time-dependent gradient of peripheral velocity to be used for spectral analysis was measured simultaneously with the two hot-film shear sensors embedded into the inner surface of the stationary outer cylinder in the test sections I and II, respectively.

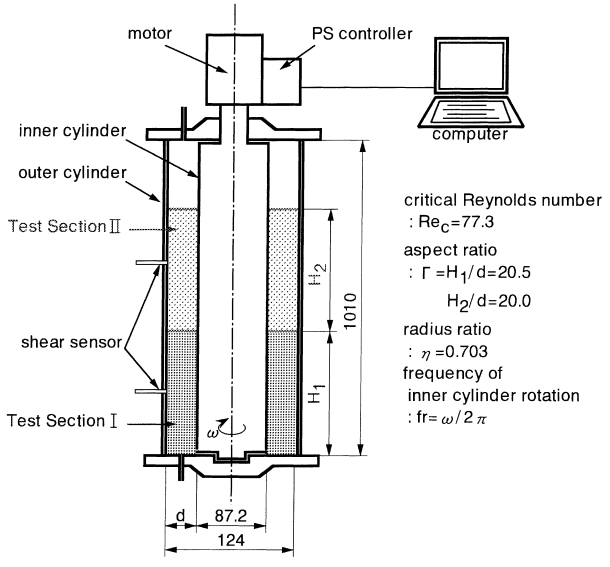

Fig. 1. Experimental apparatus. Dimensions given are in mm.

3. Results and discussion

3.1. Multiplicity of stable flow states

There appeared usually three kinds of vortex arrays, i.e. 18, 20, and 22 vortices arranged in the annulus of $\Gamma = 20.0$, depending upon the acceleration of start-up operation. The corresponding average vortex heights (termed "axial wavelength") are approximately $\lambda/d = 1.11$, 1.0 and 0.91. The larger axial wavelength $\lambda/d = 1.11$ was obtained for an impulsive start which could be realized by the computer-aided controller. Either of the two smaller axial wavelengths, i.e. $\lambda/d = 1.0$ or 0.91 appeared with probability of approximately 50% when the acceleration rate was controlled to be 0.022 rad/s^2 until reaching a specified steady operation.

As can be seen from Figs. 4 and 5, the sequential pictures of visualized cell boundaries show a remarkable difference in wave motion due to the difference in axial wavelength at the same Reynolds number.

When $\lambda/d < 1$, there appears wave motion with small amplitudes at both the inflow and outflow cell boundaries. When $\lambda/d > 1$, however, wave motion occurs at the inflow cell boundaries only. When $\lambda/d = 1$, the vortex motion is so stable that there appears only weak wave motion with very small amplitudes at both boundaries. The amplitude and time-scale $(1/f_1)$ of wave motion are smaller when $\lambda/d < 1$ than when $\lambda/d > 1$. When $\lambda/d > 1$, the amplitude of the wave motion is remarkably large at the inflow cell boundary near the inner cylinder. These suggest a difference in intercellular mass transfer coming from the difference in wave motion.

The following characteristics of Taylor vortex flow have been revealed with the observations of vortex structure and wave motion. It has been found from Fig. 6 that there can appear different stable states of wavy vortex flow in SPWVF even at the same Reynolds number. This implies that different values of effective axial diffusion coefficient can be obtained even at the same Reynolds number unless the identical start-up path is specified. The flow states can be classified into three cases, taking into account the magnitude of the first fundamental frequency.

If Re/Re_c goes beyond around 18, DPWVF becomes unstable, and its instability leads to the transition to WTWVF with the generation of chaotic turbulence superimposed on the wavy vortex flow. The turbulent motion causes a remarkable increase in inside mixing, especially in micromixing within vortex pairs.

3.2. Intercellular mass transfer

The intercellular mass transfer is suppressed at the inflow cell boundaries in the regime of LTVF. The experimental results of intercellular mass transfer are shown in the form of

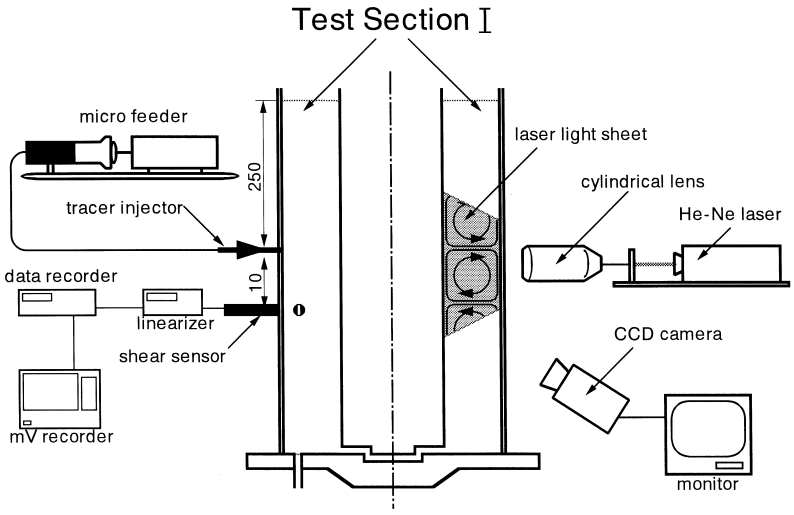

Fig. 2. Details of test section I for observation of visualized vortices.

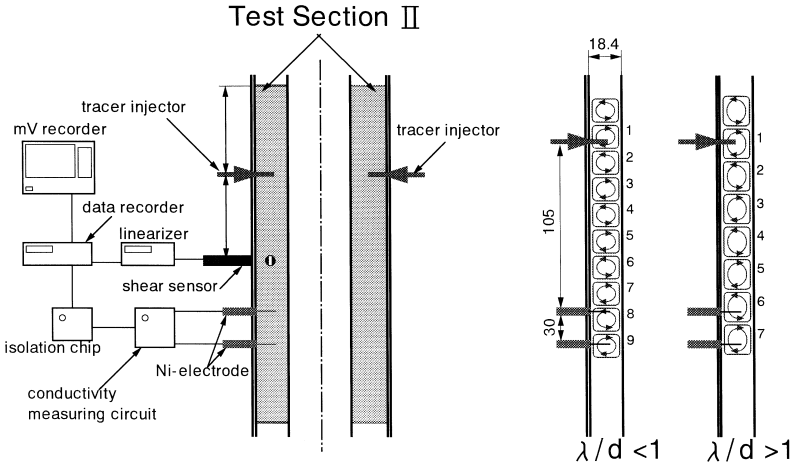

Fig. 3. Details of test section II and positioning of an inflow cell boundary.

effective axial diffusion coefficient in Fig. 7. This indicates that the intercellular mass transfer is enhanced gradually with increasing Reynolds number by the periodic wave motion of cell boundaries over the range of SPWVF and DPWVF and by the chaotic/turbulent vertical motion over the range of WTWVF and TTVF.

When $\mathrm{Re}/\mathrm{Re}_c$ goes beyond approximately 14, D_z seems to remain constant until $\mathrm{Re}/\mathrm{Re}_c = 18$. In the ranges of relatively low Reynolds number, i.e. in the range of SPWVF and DPWVF, the mass transfer over inflow cell boundaries is influenced significantly not only by the axial wavelength λ/d but also by the first fundamental frequency f_1/f_r of azimuthally traveling waves. Those effects are relatively small in the range of WTWVF and TTVF since the intercellular mass transfer is controlled mainly by turbulent mixing. That is, the fully developed turbulent vortex flow gives a very substantial axial mass transfer since the effect of turbulent mixing is prevalent over the whole flow region, not only within cellular vortices but also over cell boundaries.

As can be seen from Fig. 8, when $\lambda/d < 1$, the first fundamental frequency f_1/f_r decreases with Re in case 1 but remains almost constant in case 2. It remains constant, independent of Re in case 3, i.e. when $\lambda/d > 1$.

Taking into account the effect of the first fundamental frequency, as shown in Fig. 9, it has been found that the intercellular mass transfer is controlled not only by axial wavelength but also by the first fundamental wave motion in SPWVF and DPWVF. The Re-dependence is different, depending upon whether $\lambda/d < 1$ or not.

3.3. Intracellular mixing

The intracellular mass transfer, i.e. peripheral mass transfer inside a pair of vortices, which can be evaluated with the back-mixing coefficient E/v, is mainly controlled by the toroidal motion characteristic of Taylor vortex flow. As expected from the observation of visualized vortices (Ohmura et al., 1997b), the inside-mixing also depends on axial wavelength even in TTVF.

As shown in Fig. 10, the back-mixing was well correlated in term of the inside-mixing parameter $(E/v)(\lambda/d)$ vs. Re over the whole experimental range of Reynolds number. This implies that the intracellular mass transfer increases with Re, but that the back-mixing coefficient E/v becomes rather small when the axial wavelength is large. The inside-mixing parameter $(E/v)(\lambda/d)$ in a pair of vortices increases monotonically with Re, regardless of the flow state.

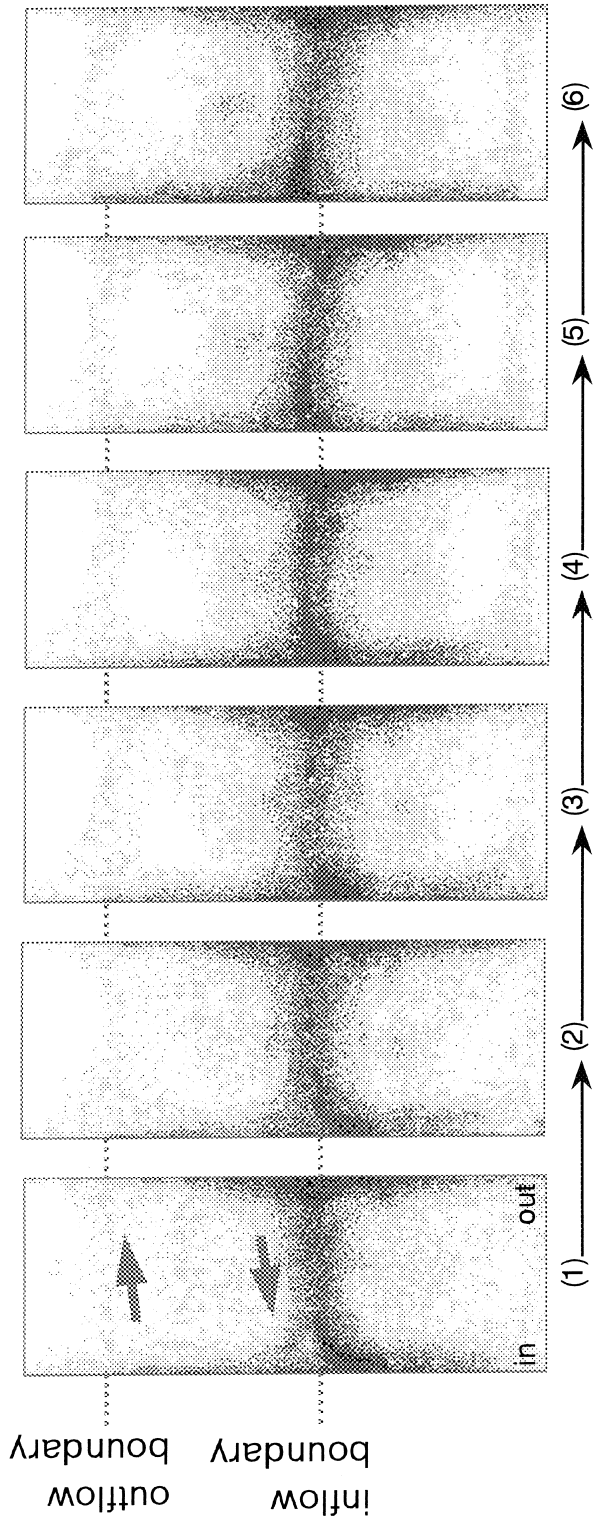

Fig. 4. Sequential pictures of wave motion of an inflow cell boundary in the case when $\lambda/d < 1$. Time interval = 0.2 s (singly periodic wavy vortex flow).

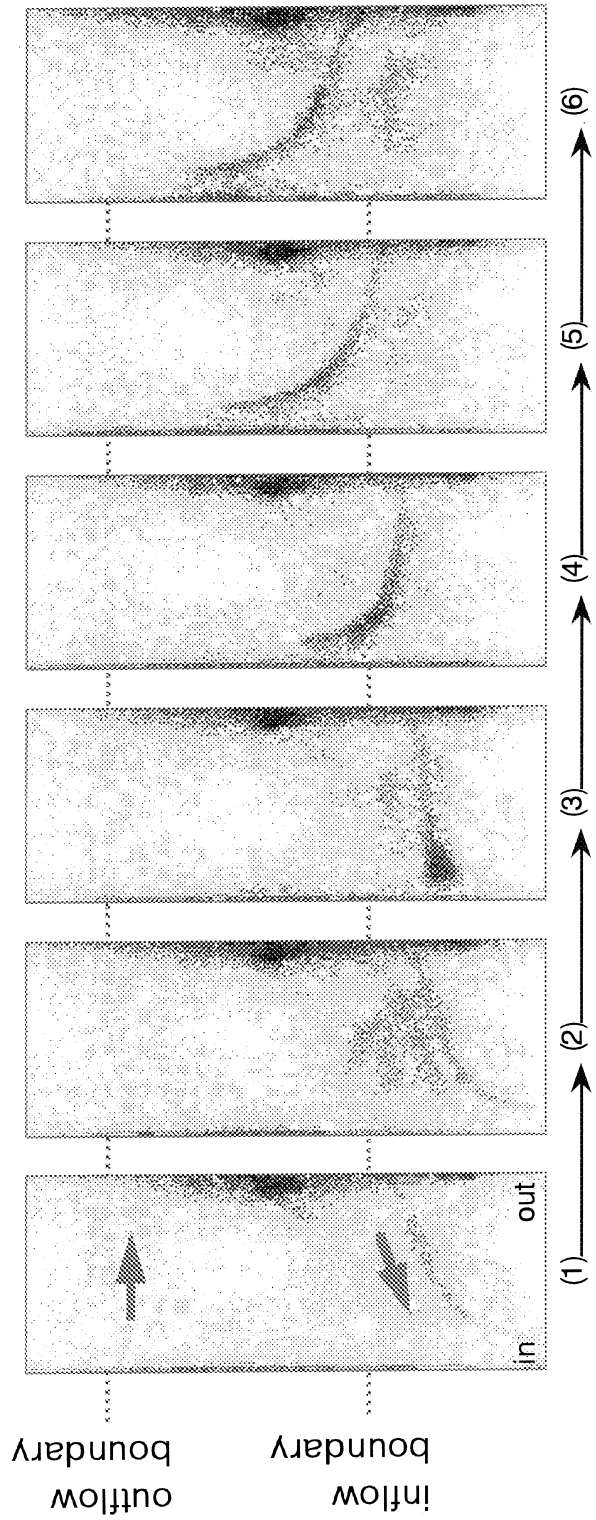

Fig. 5. Sequential pictures of wave motion of an inflow cell boundary in the case when $\lambda/d > 1$. Time interval = 0.5 s (singly periodic wavy vortex flow).

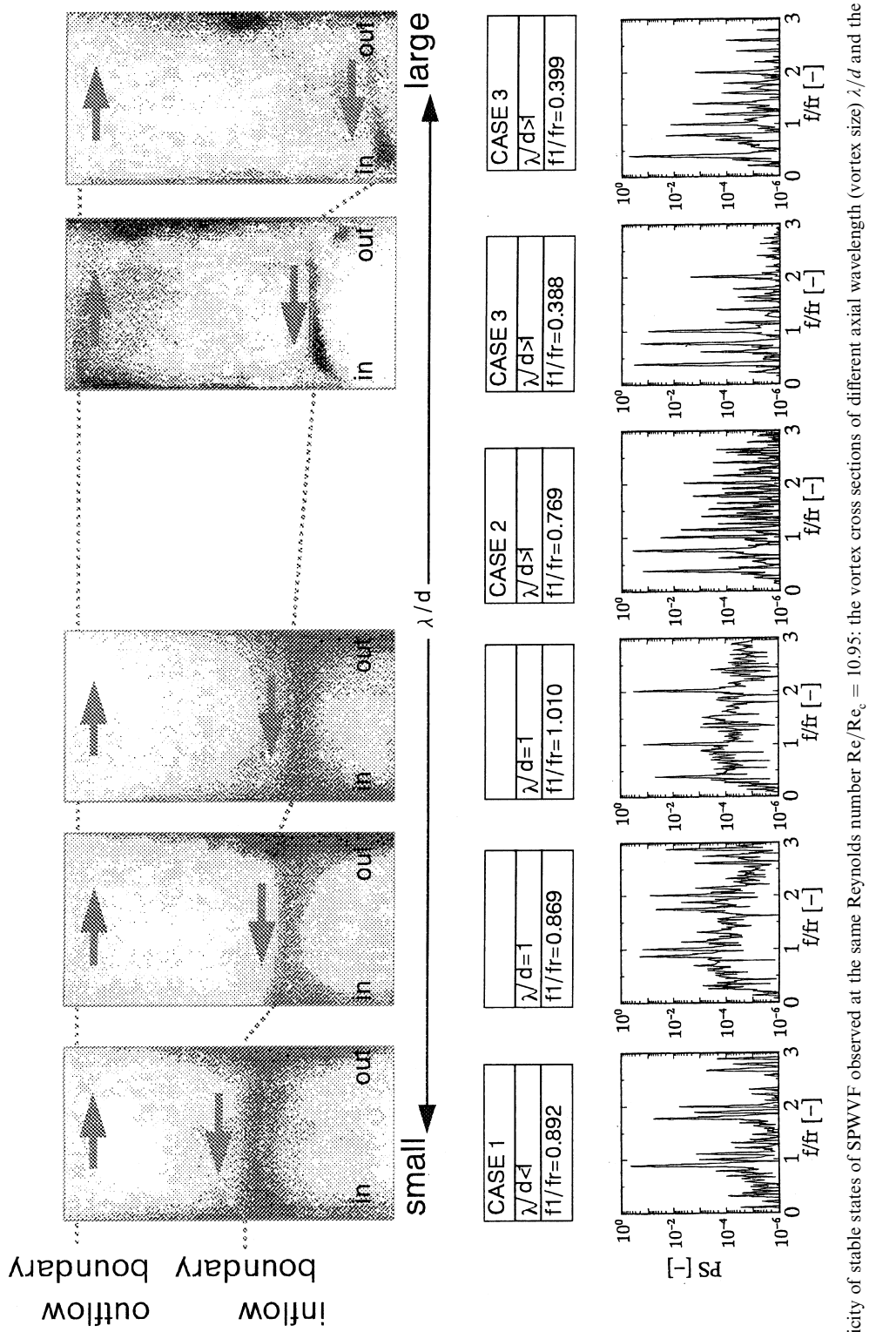

Fig. 6. Multiplicity of stable states of SPWVF observed at the same Reynolds number $Re/Re_c = 10.95$: the vortex cross sections of different axial wavelength (vortex size) λ/d and the corresponding power spectra.

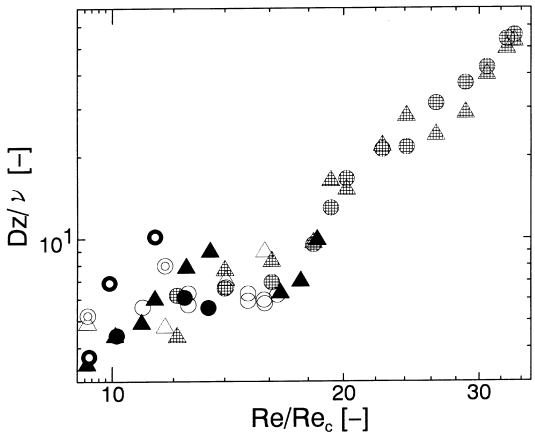

case / ν m²/s	case1	case2	case3
	λ/d < 1	λ/d > 1	
2.52x10⁻⁶	△	◍	
2.52x10⁻⁶	▲	○	●
3.05x10⁻⁶	△	◎	○

Fig. 7. Variation of effective axial diffusion coefficient with Reynolds number.

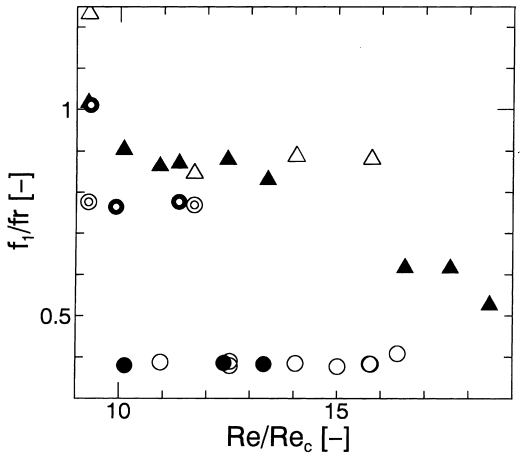

ν m²/s	case1	case2	case3
2.52x10⁻⁶	▲	○	●
3.05x10⁻⁶	△	◎	○

Fig. 8. Variation of first fundamental frequency with Reynolds number.

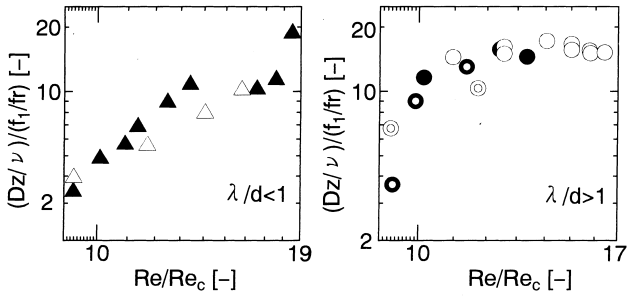

case / f_1/f_r / ν m²/s	case1	case2	case3
	0.8~1.1	0.7~0.8	0.3~0.4
2.52x10⁻⁶	▲	○	●
3.05x10⁻⁶	△	◎	○

Fig. 9. Influence of first fundamental frequency on intercellular mass transfer in the range of SPWVF and DPWVF.

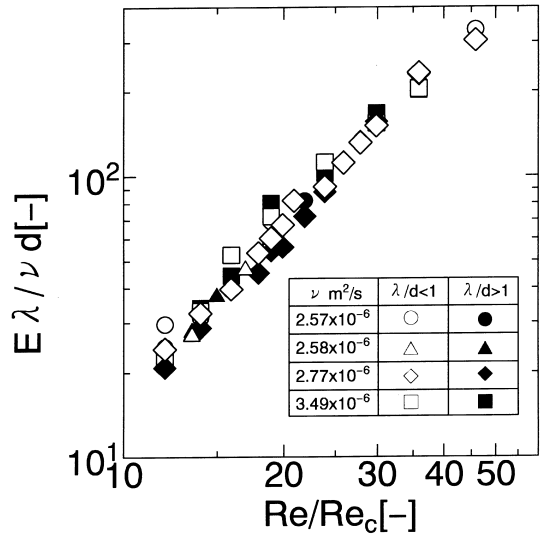

ν m²/s	λ/d<1	λ/d>1
2.57x10⁻⁶	○	●
2.58x10⁻⁶	△	▲
2.77x10⁻⁶	◇	◆
3.49x10⁻⁶	□	■

Fig. 10. Variation of back-mixing coefficient with Reynolds number.

4. Conclusions

(1) Various kinds of stable flow states can appear even at the same Reynolds number owing to the hysteresis of the flow system, depending upon the start-up operation.

(2) It is necessary to distinguish the flow states from each other taking into account the axial wavelength and first fundamental frequency in the range of SPWVF and DPWVF.

(3) The wave motions of cell boundaries differ depending not only upon the flow regime, i.e. SPWVF, DPWVF, or WTWVF, but also upon whether the axial wavelength λ/d is less than (or equal to) unity or greater than unity.

(4) Intercellular mass transfer depends upon the axial wavelength and wave motion as well as the Reynolds number in the range of SPWVF and DPWVF: the effective axial diffusion coefficient D_z/v increases primarily with increasing Re but depends also upon λ/d and f_1/f_r.

(5) Intercellular mass transfer in the range of WTWVF and TTVF is controlled mainly by turbulent motion rather than the wave motion of cell boundaries: the effects of λ/d and f_1/f_r on D_z/v are reduced by turbulent motion.

(6) Intracellular mass transfer evaluated with the inside-mixing parameter $(E/v)(\lambda/d)$ increases monotonically with Re, regardless of the flow state.

Acknowledgements

This research was supported by a Grant-in-Aid (No. 07455307) for Scientific Research (B) from the Ministry of Education, Science and Culture of Japan. The authors wish to thank Messrs. T. Yoshimura and N. Kobayashi for experimental support.

References

Kataoka, K., Doi, H., Komai, T., Futagawa, M., 1975. Ideal plug flow properties of Taylor vortex flow. J. Chem. Eng. Jpn 8, 472–476.

Kataoka, K., Takigawa, T., 1981. Intermixing over cell boundary between Taylor vortices. AIChE J. 27, 504–508.

Kataoka, K., 1986. Taylor vortices and instabilities in circular Couette flows. In: N.P. Cheremisinoff (Ed.), Encyclopedia of Fluid Mechanics, vol. 1, Chapter 9. Gulf Pub., Houston, TX, pp. 236–274.

Kataoka, K., Ohmura, N., Kamei, K., Igaki, M. 1993. Mass transfer over Taylor cell boundaries in a Taylor-Couette continuous chemical reactor. In: Proceedings of APCChE & CHEMECA 93, vol. 1, pp. 347–352.

Ohmura, N., Kataoka, K., Mizumoto, T., Nakata, M., Matsumoto, K., 1995. Effect of vortex cell structure on bifurcation properties in a Taylor vortex flow system. J. Chem. Eng. Jpn 28, 758–764.

Ohmura, N., Kataoka, K., Shibata, Y., Makino, T., 1997a. Effective mass diffusion over cell boundaries in a Taylor-Couette flow system. Chem. Eng. Sci. 52, 1757–1765.

Ohmura, N., Makino, T., Motomura, A., Shibata, Y., Kataoka, K., 1997b. Intercellular mass transfer in waving/turbulent Taylor vortex flow. In: K. Hanjalic, T.W.J. Peeters (Eds.), Proceedings of Second International Symposium on Turbulence, Heat and Mass Transfer, Delft Univ. Press, Delft, pp. 219–228.

Pudjino, P.I., Tavare, N.S., Garside, J., Nigam, K.D.P., 1992. Residence time distribution from a continuous Couette flow device. Chem. Eng. J. 48, 101–110.

Tam, Y.W., Swinney, H.L., 1987. Mass transport in turbulent Couette-Taylor flow. Phys. Rev. A 36, 1374–1391.